



HAL
open science

Development of a quantitative real-time RT-PCR assay for detecting Taiwan ferret badger rabies virus in ear tissue of ferret badgers and mice

Ai-Ping Hsu, Chun-Hsien Tseng, Yi-Ta Lu, Yu-Hua Shih, Chung-Hsi Chou, Re-Shang Chen, Kuo-Jung Tsai, Wen-Jane Tu, Florence Cliquet, Hsiang-Jung Tsai

► To cite this version:

Ai-Ping Hsu, Chun-Hsien Tseng, Yi-Ta Lu, Yu-Hua Shih, Chung-Hsi Chou, et al.. Development of a quantitative real-time RT-PCR assay for detecting Taiwan ferret badger rabies virus in ear tissue of ferret badgers and mice. *Journal of Veterinary Medical Science*, 2018, 80 (6), pp.1012-1019. 10.1292/jvms.17-0539 . anses-03409074

HAL Id: anses-03409074

<https://anses.hal.science/anses-03409074>

Submitted on 29 Oct 2021

HAL is a multi-disciplinary open access archive for the deposit and dissemination of scientific research documents, whether they are published or not. The documents may come from teaching and research institutions in France or abroad, or from public or private research centers.

L'archive ouverte pluridisciplinaire **HAL**, est destinée au dépôt et à la diffusion de documents scientifiques de niveau recherche, publiés ou non, émanant des établissements d'enseignement et de recherche français ou étrangers, des laboratoires publics ou privés.



Development of a quantitative real-time RT-PCR assay for detecting Taiwan ferret badger rabies virus in ear tissue of ferret badgers and mice

Ai-Ping HSU^{1,2)}, Chun-Hsien TSENG¹⁾, Yi-Ta LU¹⁾, Yu-Hua SHIH^{1,2)}, Chung-Hsi CHOU^{2,3)}, Re-Shang CHEN^{1,2)}, Kuo-Jung TSAI¹⁾, Wen-Jane TU¹⁾, Florence CLIQUET⁴⁾ and Hsiang-Jung TSAI^{2,3)*}

¹⁾Animal Health Research Institute, Council of Agriculture, No.376, Zhong zheng Rd., Tamsui Dist., New Taipei City 251, Taiwan (R.O.C.)

²⁾Graduate Institute of Veterinary Medicine, School of Veterinary Medicine, National Taiwan University, No. 1, Sec. 4, Roosevelt Rd., Taipei 106, Taiwan (R.O.C.)

³⁾Zoonoses Research Center, School of Veterinary Medicine, National Taiwan University, No. 1, Sec. 4, Roosevelt Rd., Taipei 106, Taiwan (R.O.C.)

⁴⁾Nancy OIE/WHO/EU Laboratory for Rabies and Wildlife, French Agency for Food, Environmental and Occupational Health & Safety, Technopole Agricole et Vétérinaire de Pixérécourt, Bâtiment H, CS 40009, 54220 MALZEVILLE, France

ABSTRACT. In 2013, the first case of Taiwan ferret badger rabies virus (RABV-TWFB) infection was reported in Formosan ferret badgers, and two genetic groups of the virus were distinguished through phylogenetic analysis. To detect RABV-TWFB using a sensitive nucleic acid-based method, a quantitative real-time reverse transcription polymerase chain reaction targeting the conserved region of both genetic groups of RABV-TWFB was developed. This method had a limit of detection (LOD) of 40 RNA copies/reaction and detected viral RNA in brain and ear tissue specimens of infected and dead Formosan ferret badgers and mice with 100% sensitivity and specificity. The mean viral RNA load detected in the ear tissue specimens of ferret badgers ranged from 3.89×10^8 to 9.73×10^8 RNA copies/g-organ, which was 111-fold to 2,220-fold lower than the concentration detected in the brain specimens, but 2,000-fold to 5,000-fold higher than the LOD of the assay. This highly sensitive technique does not require facilities or instruments complying with strict biosafety criteria. Furthermore, it is efficient, safe, and labor-saving as only ear specimens need be sampled. Therefore, it is a promising technique for epidemiological screening of Taiwan ferret badger rabies.

KEY WORDS: rabies diagnosis, real-time RT-PCR, Taiwan ferret badger rabies

J. Vet. Med. Sci.

80(6): 1012–1019, 2018

doi: 10.1292/jvms.17-0539

Received: 27 December 2017

Accepted: 4 April 2018

Published online in J-STAGE:
30 April 2018

Rabies is a major and lethal zoonotic disease that is spread mainly through bites inflicted by rabid animals. The etiological agents responsible are rabies viruses, which belong to the family *Rhabdoviridae*, and the genus *Lyssavirus*. In developed countries, rabies prevention strategies have been introduced, and public health awareness has improved, but the threat has not been eliminated. Recent cases of human rabies in developed countries have been attributed to bats and wild carnivores, such as foxes and raccoon dogs in Europe, or raccoons and skunks in North America [6, 9].

The first rabies case reported in Formosan ferret badgers (*Melogale moschata subaurantiaca*) in Taiwan was in 2013 [23]. Since then, the rabies status in Taiwan has changed, and the Taiwan government has implemented a program of constant surveillance and diagnosis. From 2013 until the end of 2016, of 6,626 tested animals (including 1,869 wild carnivores), 553 Formosan ferret badgers (553/561, 98.57%), 6 Formosan gem-faced civets (*Paguma larvata taivana*), a dog (*Canis familiaris*) and a shrew (*Suncus murinus*) from nine Taiwanese counties were identified as being rabies-positive [3]. Phylogenetic studies have inferred the presence of two major genetic groups of the virus at different geographical locations in Taiwan; the TW-I group in the western part, and the TW-II group in the eastern part, with the 3,000-m high Central Mountain Range acting as a natural barrier [18].

Accurate diagnostic techniques are essential tools for the surveillance and control of rabies. An ideal diagnostic technique should have satisfactory sensitivity and specificity. The sensitivity of the fluorescent antibody test (FAT), for example, can be as high as

*Correspondence to: Tsai, H.-J.: tsaihj@ntu.edu.tw

©2018 The Japanese Society of Veterinary Science



This is an open-access article distributed under the terms of the Creative Commons Attribution Non-Commercial No Derivatives (by-nc-nd) License. (CC-BY-NC-ND 4.0: <https://creativecommons.org/licenses/by-nc-nd/4.0/>)

99% in laboratories with experienced personnel [14]. The other two conventional reference diagnostic methods, which are based on virus propagation and isolation, are the mouse inoculation technique (MIT) and the rabies tissue culture infection test (RTCIT) [12, 22, 24]. Although viral amplification can facilitate downstream molecular analyses, a definitive diagnosis is generally time-consuming [10, 14]. In addition, to apply these diagnostic techniques, laboratories must be equipped with cell culture facilities, fluorescent microscopy instruments, necropsy facilities, or animal housing resources that meet biosafety criteria.

Diagnostic techniques based on nucleic acid amplification and detection have various advantages over conventional rabies diagnostic techniques like FAT, MIT, and RTCIT, with the most prominent advantage being higher sensitivity [14, 15, 20]. For example, it was previously reported that viral titers as low as $10^{-5.93}$ mouse intracranial median lethal dose (MICLD₅₀) or 0.02 median tissue culture infectious dose (TCID₅₀/ml) were detectable [2, 16]. Low detection thresholds increase the potential nucleic-acid amplification based techniques, enabling the analysis of samples containing a small quantity of viral RNA for peripheral diagnosis by using fluid samples such as saliva, cerebrospinal fluid, tears, and urine, and avoiding the need to open the skull [2, 8, 17, 19, 20].

In the present study, we developed a TaqMan real-time reverse transcription-polymerase chain reaction (RT-PCR) assay to detect Taiwan ferret badger rabies virus (RABV-TWFB) in the ear tissues of infected ferret badgers. Our primers and probes were designed to target the conserved region of the nucleoprotein (N) gene of RABV-TWFB in both the TW-I and TW-II groups. Our main aim was to develop and validate a technique using peripheral tissues such as ear tissue, thus avoiding the need to sample the ferret badger brains, thereby facilitating a primary screening method applicable to epidemiological surveys. The results demonstrated that this real-time RT-PCR assay was extremely sensitive, and should benefit the epidemiological screening of RABV-TWFB in Taiwan ferret badgers.

MATERIALS AND METHODS

Animal specimen sources and ethics statements

The animal sources for all the specimens used in the current study were not collected exclusively for this study, but were originally used for semi-lethal dose titration, pathogenicity research, or vaccine evaluation of RABV-TWFB. To remain compliant with the Three Rs concept (i.e., replacement, reduction, and refinement), paired ear and brain tissues of euthanized field animals from the aforementioned experiments were collected for further evaluation in the current study. All the animal experiments and protocols were approved by the Institutional Animal Care and Use Committee (IACUC) of the Animal Health Research Institute, Taiwan (permit nos. IACUC# A03031, A04019 and A05005).

Formosan ferret badgers weighing approximately 1 kg each were captured in Miaoli County, Taiwan, which is a rabies-free zone. Before the experiments, each ferret badger was micro-chipped for individual identification and isolated for more than six months for observation to confirm the absence of rabies; the absence of rabies virus-neutralizing antibodies was confirmed by using a fluorescent antibody virus neutralization test [5]. The mice used for this study were specific pathogen free BALB/c mice aged 3–4 weeks from National Laboratory Animal Center, Taipei City, Taiwan.

All inoculations were conducted when the animals were effectively anesthetized to suitably levels using isoflurane at 1–4% by inhalation. Respiration, heart rate, and pain reflexes were monitored during the virus inoculations. At the onset of clinical signs indicating rabies, or at the end of the experiments, all the mice and ferret badgers were humanely euthanized using 5% isoflurane for 1 min after the heart beating and breathing had stopped. It was decided that animals would be euthanized at the onset of clinical signs suggestive of rabies in order to prevent unnecessary animal suffering.

Rabies virus inoculations

Thirty mice and 14 ferret badgers were experimentally infected with TW-II RABV-TWFB (TW-II-mice and TW-II-FB, respectively). Fourteen mice were infected with TW-I RABV-TWFB (TW-I-mice). Ten uninfected mice and ten uninfected ferret badgers served as negative controls for evaluation of the specificity of the assay. The two stains of RABV-TWFB used for animal inoculations were salivary gland preparations derived from rabid ferret badgers collected in 2014 from Western or Eastern Taiwan, and assigned as RABV-TWFB-I and RABV-TWFB-II, respectively. The sequencing results confirmed that both viruses had identical nucleotide sequences to the primers and probe designed in the current study. RABV-TWFB-I was intracranially inoculated into the mice at a dose of $10^{1.2}$ (n=6), $10^{0.7}$ (n=5) or $10^{0.2}$ (n=3) MICLD₅₀. RABV-TWFB-II was intracranially inoculated into the mice at a dose of $10^{2.7}$ (n=6), $10^{1.7}$ (n=6), $10^{1.4}$ (n=7), $10^{1.1}$ (n=7) or $10^{0.7}$ (n=4) MICLD₅₀. RABV-TWFB-II was injected intramuscularly into the Formosan ferret badgers at $10^{3.9}$ (n=4), $10^{3.1}$ (n=3), $10^{2.3}$ (n=4) or $10^{1.5}$ (n=3) MICLD₅₀.

Tissue suspensions and RNA preparation

In total, 54-mouse and 24-ferret badger brain and ear specimens were each collected. To obtain the ear specimens, bilateral whole-ear tissues from each mouse and a specimen piece of approximately 1×1 cm from the apical margin of one ear from each ferret badger were collected. The tissues were minced using sterile scissors. After the tissue samples had been ground and prepared as 10% tissue suspensions in Dulbecco's modified Eagle's medium (Gibco, Grand island, NE, U.S.A.), the RNA was extracted using an automatic nucleic acid extraction system (taco™; GeneReach, Taichung, Taiwan R.O.C.) with a taco Preloaded DNA/RNA Extraction Kit (GeneReach). Briefly, after clarification of the tissue suspension by full-speed centrifugation for 10 min at 4°C, 140 μ l of the supernatant was used for extraction. The RNA elution samples (200 μ l) were recovered and stored at -80°C until analysis.

Table 1. Detailed information on the primers and probe used

Primer/ probe	Name	Application in this study	Sequence (5'→3')	Genome position
Primer	TW-RAV-F	Real-time RT-PCR	GATGCTATATGGGTCAAGTCAGATCTC	1,017–1,043
	TW-RAV-R	Real-time RT-PCR	CTGCCAATGCCACATCAG	1,217–1,200
	TW-RAV-F- <i>Hind</i> III	Optimization for complete plasmid linearization	AATTC AAGCTTGATGCTATATGGGTCAAGT	Artificial
	TW-RAV-R- <i>Spe</i> I	Optimization for complete plasmid linearization	TTAAGACTAGTCTGCCAATGCCACATCAGT	Artificial
Probe	TW-RAV-FAM	Real-time RT-PCR	FAM-ATGTCTGTTCTGGGAGGCTA-BHQ-1	1,082–1,101

Primers and probe designs

The N gene sequences for ten RABV-TWFB strains, according to the whole-genome sequences first reported in 2013 [1], were used to design gene-specific primers and the probe. The N gene sequences of the ten strains, with accession numbers KF501180, KP881353, KF501181, KP881355, KF501182, KF501183, KP881354, KP881356, KF501184 and KF501185, were extracted from GenBank. Of these sequences, KF501180 and KP881353 belonged to the TW-II group isolated from Eastern Taiwan, whereas the remaining eight were from the TW-I group isolated from Western Taiwan [18]. Three identical stretches of nucleotide sequence were identified among the N gene sequences of the ten virus strains. These sequences were used for the primer set and the probe used to generate and screen for the amplicon of 201 nucleotides, using the TaqMan real-time RT-PCR assay. The two strains of viruses used for animal inoculations were demonstrated to have the same nucleotide sequences as the primers and probe. The probe was labeled with fluorescent reporter dye 6-carboxy-fluorescein (FAM) at the 5'-end, and 6-carboxytetramethylrhodamin at the 3'-end (Biosearch, Novato, CA, U.S.A.). Table 1 shows the detailed sequence information for the primers and probe used. The identities of the N gene sequences derived from 63 RABV-TWFB strains published by Chiou *et al.* [4] and Tsai *et al.* [18] were compared in the regions of our primers and the probe by using the multiple-alignment functions of DNASTAR[®] software (DNASTAR, Madison, WI, U.S.A.).

Plasmid construction and generation of RNA standards

The sequences of the ten RABV-TWFB strains were all identical to our primer set and probe. To produce a plasmid for use in the generation of standard control RNA, DNA fragments spanning within the target amplicon defined by the primers TW-RAV-F and TW-RAV-R were produced using the SuperScript[®] III One-Step RT-PCR System (Invitrogen, Waltham, MA, U.S.A.) with one of the viral RNA samples (strain KF501185), and the primer pair (TW-RAV-F and TW-RAV-R) according to the manufacturer's instructions. The thermal cycling profile was comprised of one cycle of 50°C for 20 min; 35 sequential cycles of 94°C for 10 sec, 50°C for 20 sec, and 68°C for 1 min, followed by a final extension at 68°C for 10 min. The recovered PCR products were cloned to a pCRII-TOPO[®] vector (Invitrogen) as per the manufacturer's instructions. The clone possessing the target sequence in the orientation of the minus strand downstream from the T7 promoter was selected, based on sequencing results. To ensure the subsequent linearization process, an optimizing fragment amplified using the primer pair TW-RAV-F-*Hind* III and TW-RAV-R-*Spe* I was cloned into the aforementioned plasmid downstream of the fragment amplified by the TW-RAV-F and TW-RAV-R primers. After mini-preparation using the QIAprep Spin Miniprep Kit (Qiagen, Hilden, Germany), the plasmid was further double-cut by digestion using *Hind* III and *Spe* I to generate a fully linearized plasmid. Following linearization, electrophoresis was used to separate the linearized plasmid from the optimizing fragment, and gel extraction used to isolate the fully linearized plasmid. The linearized plasmid fragment served as the template for generating the minus-stranded RNA standard using the T7 RiboMAX[™] Express Large Scale RNA Production System Kit (Promega, Fitchburg, MA, U.S.A.). After DNase treatment and purification with RNeasy[®] MinElute[®] Cleanup (Qiagen), the RNA concentration was quantified using a NanoPhotometer (Implen, Munich, Germany).

Detection and quantification of RABV-TWFB RNA using a one-step real-time RT-PCR

Nucleic acid was amplified using real-time RT-PCR on a Roche LightCycler[®] 480 II (Roche, Basel, Switzerland) using a KAPA PROBE FAST Universal One-step qRT-PCR Kit (Kapa, Cape Town, South Africa). A 20 µl reaction mixture composed of 0.4 µl of KAPA RT Mix (50 ×), 10 µl of KAPA Probe Fast qPCR Master Mix (2×), 3 µl of RNA sample, 400 nM final concentrations of each primer and 500 nM of probe. The thermal cycling profile was as follows: a single stage for reverse transcription at 42°C for 20 min and reverse transcriptase inactivation at 95°C for 5 min, followed by 50 sequential cycles of 95°C for 3 sec and 60°C for 35 sec. Fluorescent signals were detected at the end of the elongation phases. According to the automatic calculation by the LightCycler[®] 480 software, based on the second derivative maximum method, the time when the fluorescence curve of sample RNA turned sharply upward was automatically recorded as the crossing point (Cp) for a specific RNA concentration. Ten-fold serial dilutions of the RNA standard with a 10-log range of concentration from 9.6 × 10¹⁰ to 96 copies/reaction in diethylpyrocarbonate (DEPC)-treated water were used as template. The measurement of the Cp values were performed in quintuplicate and used to create a dedicated standard curve. To determine whether the standard curve was appropriate for quantifying the RNA copy numbers extracted from the brain and ear specimens (where the presence of RNA inhibitors was a concern), four regression lines were created. In these, the T7 RNA transcripts were separately suspended in a background of RNA extracted from the brain or ear emulsions of rabies-negative mice or ferret badgers. Briefly, 10-fold serial dilutions of the RNA standards with a 10-log range of concentration (9.6 × 10¹⁰ to 96 copies/reaction) were mixed with the extracted RNA prepared from rabies-negative specimen mixtures of 15 ferret badger brain samples, 15 ferret badger ear samples, eight mouse brain samples, or

eight mouse ear samples. These samples were then submitted for Cp measurement in quintuplicate to create the regression lines for statistical comparison with the dedicated standard curve. Each RNA sample was analyzed in triplicate, and in every independent analysis run, a standard RNA sample, of a known concentration was included (also in triplicate) and served as a calibrator. Quantifications and concentration calculations for the RNA samples extracted from the brain and ear specimens of rabies-positive ferret badgers were conducted based on the standard curve and the built-in function of the LightCycler® 480.

Data analysis

The standard curve was estimated according to the error value and efficiency (E), $E=10^{(-1/\text{slope})}$, which was automatically calculated by the LightCycler® 480 software. To determine the limit of detection (LOD), 10-fold RNA standards at 10–100 copies/reaction were analyzed in at least 20 replicates to assess the positive detection rate for each concentration. An LOD was assigned as the concentration with a Cp at which $\leq 5\%$ of the true-positive standard RNA was found to be negative. To compare the four regression lines (generated from the T7 RNA transcripts suspended and diluted in the background of extracted RNA derived from the brain or ear emulsions of the rabies-negative mice or ferret badgers) with the dedicated standard curve (T7 RNA transcripts suspended in RNase-free water), an analysis of covariance (ANCOVA) with a 95% confidence interval was conducted using SAS 9.4 software (SAS, Cary, NC, U.S.A.). An RNA sample was considered positive if fluorescent signals were detected in all three wells, and the average Cp of the triplicate values was less than the upper limit Cp of the LOD (average value added to $1.96 \times$ standard deviations). Sensitivity and specificity were compared with FAT results, which were set as the gold standard. Statistical comparisons of the RNA copy numbers extracted from ferret badgers receiving different virus dilutions were first analyzed using the Shapiro-Wilk test to confirm distribution normality, and then the mean or median RNA copy numbers detected were compared using one-way analysis of variance (ANOVA) or the Kruskal–Wallis test using the SAS 9.4 software.

RESULTS

Multiple alignments of published sequences

Out of 63 published N gene sequences derived from RABV-TWFB, 54 had completely identical nucleotide sequences in the regions of the primers and probe used in this study (54/63, 85.7%). Six TW-I-group viral strains possessed one nucleotide difference in the forward primer region (6/63, 9.5%), while one TW-II-group viral strain had one nucleotide mismatch in the reverse primer region (1/63, 1.6%). One TW-II-group viral strain had two nucleotide differences in the reverse primer region (1/63, 1.6%). Only one viral strain (KP860178, TW-II group) was shown to carry three nucleotide mismatches, with one each being located in the two primer regions, and the third being within the region of the probe (1/63, 1.6%). The alignment results are displayed in Fig. 1.

Generation of the standard curve, LOD determination, and comparison of the dedicated standard curve with the regression lines from template in a background of potential PCR inhibitors

The standard curve regression analyzed using the LightCycler®480 showed satisfactory results, with the error value being 0.0181 (below 0.2, which is acceptable according to the LightCycler®480's test criteria), and an E value of 1.981, indicating that this assay was suitable for quantifying RABV-TWFB RNA samples (Fig. 2).

The LOD tests revealed that concentrations >40 copies/reaction resulted in $\geq 95\%$ positive detection. Thus, our assay had a LOD of 40 RNA copies/reaction or 13.33 RNA copies/ μl of RNA sample, which is equivalent to approximately 1.90×10^5 RNA copies/g of organ tissue. This indicated a Cp of 38.49 was an appropriate cut-off point for determining whether a sample was positive or negative (Table 2).

To clarify whether the RNA copy number of the RNA samples extracted from the brain and ear specimens could be calculated based on the standard curve created with the T7 RNA transcript suspended in the RNase-free water, ANCOVA tests were performed. The results revealed no significant differences in the comparisons of the slopes between the standard curve and the four regression lines ($P=0.97, 0.98, 0.98$ and 0.98 ; Fig. 3), or between the Y intercepts of the standard curve and the four regression lines ($P=0.76, 0.84, 0.94$ and 0.77 ; Fig. 3). This indicated that no concerns existed regarding the effects of any PCR inhibitors present in the samples extracted from the brain or ear specimens on the accuracy of RNA quantitation.

		Forward primer	Reverse primer	Probe
Consensus sequence		GATGCTATATGGGTCAAGTCAGATCTC	CTGCCAATGOCACATCAG	ATGTCTGTCTCTGGGAGGCTA
KP860141	TW-IT.....
KP860143	TW-IT.....
KP860145	TW-IT.....
KP860146	TW-IT.....
KP860160	TW-IC.....
KP860161	TW-IC.....
KP860181	TW-IIC.....G.....T
KP860162	TW-IIC.....G.....
KP860178	TW-IIC.....G.....T.....

Fig. 1. Comparison of nucleotide mismatches in the primer and probe regions. The consensus sequences denote identity with our primer or probe sequences; 54 of the 63 published strains are denoted with dots (*). Of the 63 published strains, KP860141, KP860143, KP860145, KP860146, KP860160, KP860161, KP860181, KP860162 and KP860178 showed mismatches in the primer and probe regions. Among these nine strains, KP860141, KP860143, KP860145, KP860146, KP860160 and KP860161 were classified as the TW-I group, while KP860181, KP860162, and KP860178 were classified as the TW-II group.

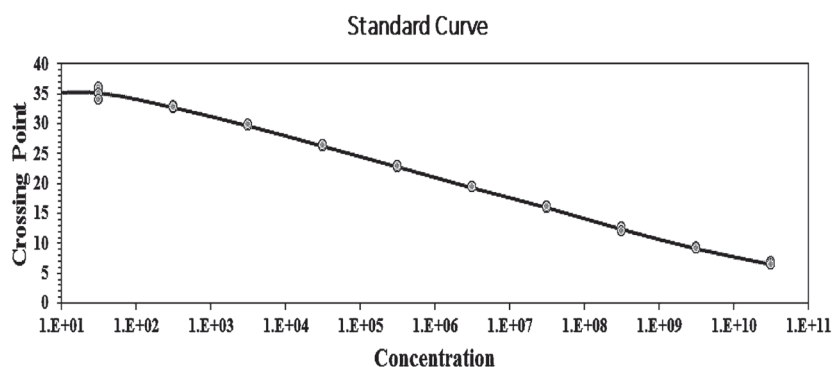


Fig. 2. Generation of the standard curve. A 10-log range of concentrations provided a satisfactory standard curve with an error value of 0.0181 and E value of 1.981.

Table 2. Real-time RT-PCR assay limit of detection determination

Standard RNA concentration, copies/reaction (copies/g-organ)	Well numbers of tested positive/replicates of well numbers (%)	Upper value of Cp
100 (4.76×10^5)	20/20 (100)	- ^{a)}
90 (4.29×10^5)	20/20 (100)	-
80 (3.81×10^5)	20/20 (100)	-
70 (3.33×10^5)	30/30 (100)	37.55
60 (2.86×10^5)	40/40 (100)	37.60
50 (2.38×10^5)	38/40 (95.0)	37.88
40 (1.90×10^5)	39/40 (97.5)	38.49
30 (1.43×10^5)	43/50 (86.0)	38.21
20 (9.52×10^4)	30/40 (75.0)	38.64
10 (4.76×10^4)	23/40 (57.5)	38.92

a) Not calculated.

Sensitivity and specificity of the real-time RT-PCR assay

Brain and ear specimens from 54 mice and 24 ferret badgers experimentally infected with either TW-I or TW-II RABV-TWFB, or non-infected controls, were analyzed using the real-time RT-PCR assay. We observed 100% positive detection rates for both the brain and ear specimens derived from the TW-II-FB, TW-I-mice, and TW-II-mice, consistent with the FAT results, thus indicating that the assay was 100% sensitive. In addition, the real-time RT-PCR results of both the brain and ear specimens derived from all FAT-negative mice and ferret badgers were also negative, indicating 100% specificity as well (Table 3).

Quantification and comparison of RNA copies of RABV-TWFB derived from brain and ear specimens from rabies-positive ferret badgers

To determine whether the ear tissue samples from ferret badgers were able to serve as the target specimens for rabies diagnosis, the viral RNA copies extracted from the brain and ear tissue samples were quantified and compared. To determine the exact viral RNA copies extracted from the brains and ears of ferret badgers infected with RABV-TWFB-II, viral RNA copies were quantified using the real-time RT-PCR assay developed and described herein (Fig. 4). The Kruskal–Wallis and ANOVA analyses with a 95% confidence interval demonstrated that there were no significant differences in the viral RNA copy-number detected in either brain or ear specimens from ferret badgers receiving different virus doses (MICLD₅₀ titers of $10^{3.9}$, $10^{3.1}$, $10^{2.3}$ and $10^{1.5}$; $P=0.69$ and 0.60, respectively). The highest viral RNA load detected from ferret badger brain and ear was 5.35×10^{11} and 1.90×10^9 , respectively, and the lowest was 1.50×10^{10} and 6.76×10^6 RNA copies/g-organ, respectively (Fig. 4A and 4B). The median viral RNA copy-number detected from ferret badger brain samples was in the range of 1.21×10^{11} (interquartile range, 8.67×10^{10} – 1.32×10^{11}) to 2.80×10^{11} (range, 1.48×10^{11} – 4.08×10^{11}) RNA copies/g-organ. The mean viral RNA copy-number detected from ferret badger ears was in the range of $3.89 \times 10^8 \pm$ standard deviation (SD) 5.66×10^8 to $9.73 \times 10^8 \pm$ SD 7.47×10^8 RNA copies/g-organ (Fig. 4A and 4B).

The detected viral RNA load ratios of brain:ear (viral RNA copies in the brain:viral RNA copies in the ear) are displayed in Fig. 4C. The Kruskal–Wallis test also revealed no significant differences in the ratios between ferret badgers receiving virus at MICLD₅₀ titers of $10^{3.9}$, $10^{3.1}$, $10^{2.3}$, and $10^{1.5}$ ($P=0.27$); therefore, when ferret badgers were intramuscularly infected with RABV-TWFB-II with $10^{1.5}$ – $10^{3.9}$ MICLD₅₀, the median ratio of viral RNA copies brain:ear was in the range of 111 (range, 75.40–1,630) to 2,220 (range, 1,370–2,270; Fig. 4C).

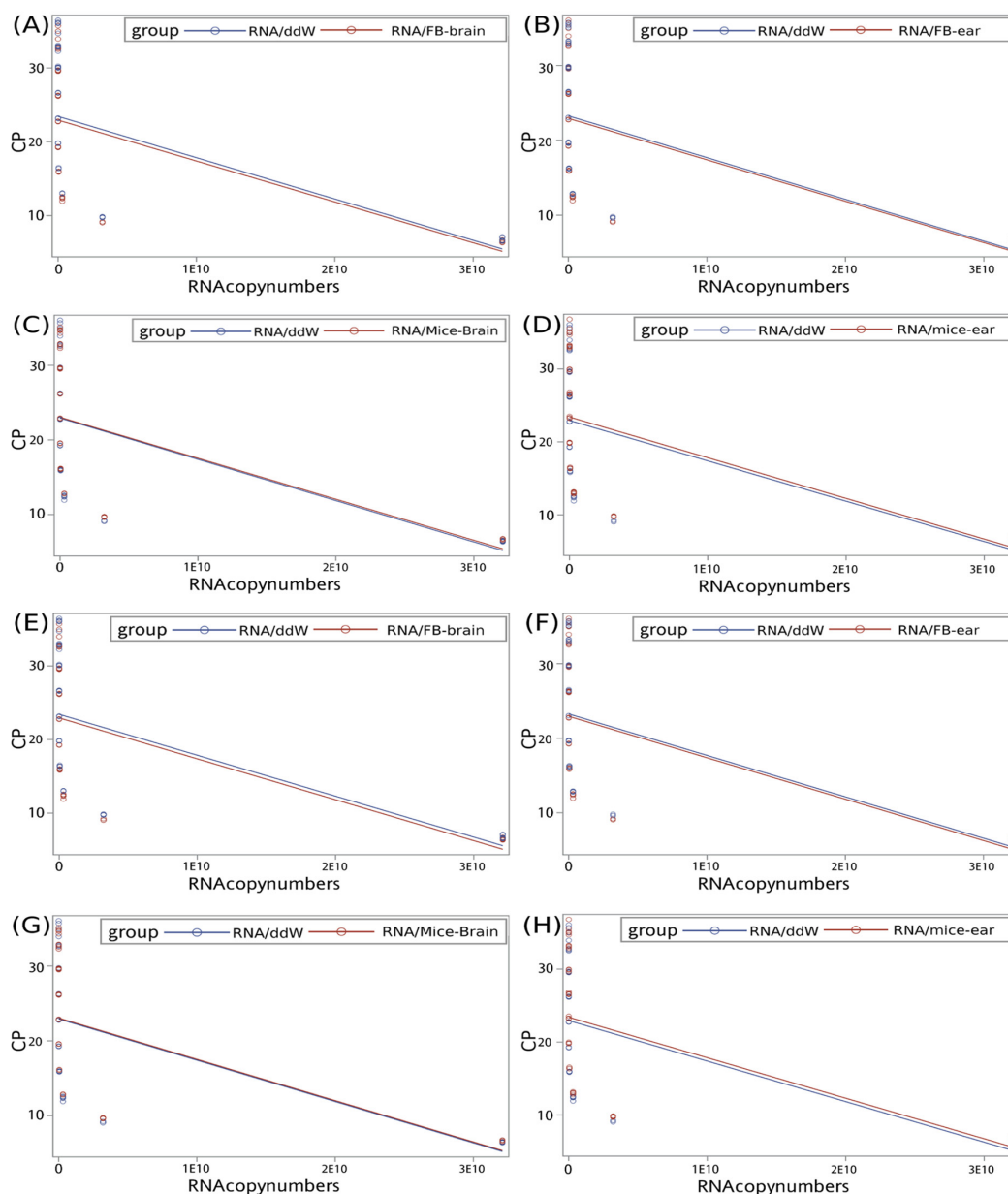


Fig. 3. Analysis of covariance between the standard curve and the regression line in the background of potential PCR inhibitors. The analysis of covariance was determined by evaluating the slopes (A) to (D) and Y intercepts (E) to (H) between the standard curve and the individual regression lines created using a background of RNA derived from ferret badger brains, ferret badger ears, mouse brains, or mouse ears. All analyses revealed insignificant differences with *P* values of 0.97, 0.98, 0.98, 0.98, 0.76, 0.84, 0.94 and 0.77 for (A) through (H), respectively. RNA/ddW, RNA/FB-brain, RNA/FB-ear, RNA/mouse-brain, and RNA/mouse-ear, represent the RNA transcripts suspended and serially diluted in DEPC water, RNA extraction of ferret badger brain specimens, RNA extraction of ferret badger ear specimens, RNA extraction of mouse brain specimens, and RNA extraction of mouse ear specimens, respectively.

Table 3. Real-time RT-PCR assay sensitivity and specificity evaluation

	Brain specimens		Ear specimens	
	Number of PCR positive/ number of FAT positive (%)	Number of PCR negative/ number of FAT negative (%)	Number of PCR positive/ number of FAT positive (%)	Number of PCR negative/ number of FAT negative (%)
TW-II-FB	14/14 (100)	- ^{a)}	14/14 (100)	-
TW-I-mice	14/14 (100)	-	14/14 (100)	-
TW-II-mice	30/30 (100)	-	30/30 (100)	-
Negative ferret badgers	-	10/10 (100)	-	10/10 (100)
Negative control mice	-	10/10 (100)	-	10/10 (100)

a) Not applicable.

DISCUSSION

When rabies infections in Formosan ferret badgers were first discovered in Taiwan in 2013, a huge number of animals had to be tested within a short period. The rabies diagnosis workload ballooned to between 5-fold and 10-fold the average from the decade preceding the discovery [3]. A proposal was made to develop effective and accurate screening tests that do not need instruments and facilities requiring strict compliance with biosafety criteria, and then to appoint certain competent laboratories to conduct the primary screening. In the current study, a highly sensitive real-time RT-PCR assay based on easily collectable peripheral tissues of ferret badgers (i.e., ear tissue) was thus developed. It has been demonstrated in this study that the amount of viral RNA detected in brain tissues was several hundred-fold to a thousand-fold higher than that detected in ear tissues. Therefore, if peripheral tissues such as skin or ears can provide an accurate diagnosis compared with conventionally tested brain specimens, the diagnostic technique should be considered sufficiently sensitive. As shown in this study, the mean concentration of viral RNA detected in ear specimens from the TW-II-FB group using the TaqMan real-time RT-PCR was $3.89\text{--}9.73 \times 10^8$ RNA copies/g-organ, which was approximately 2,000-fold to 5,000-fold higher than the LOD of the assay.

Studies have been used to developed efficient nucleic acid-based techniques for human rabies diagnosis using saliva and nuchal skin biopsy specimens [7, 8, 13], which are useful for special purposes such as ante-mortem examination before administering treatments, or for screenings associated with organ transplantation. These techniques are also applicable to several animal species such as dogs, cats, mongooses, and goats [25]. The current study is the first to demonstrate that ferret badger ear tissue, a peripheral tissue, is suitable for rabies diagnosis using a nucleic acid-based technique, which was validated to have a sensitivity and a specificity of 100% each compared with FAT as a reference method. A higher sensitivity was obtained in this study compared to previous studies using nucleic acid detection to test human skin biopsies [8, 13] or the muzzle skin of different animal species [25]. Although we did not investigate the performance of this real-time RT-PCR on ferret badgers infected by RABV-TWFB-I, the sensitivity evaluation on the ears of TW-I-mice also attained 100%, so this technique may be applied to both RABV-TWFB genetic groups in Taiwan.

A key factor affecting the sensitivity of a real-time RT-PCR assay is the identity between the primer or probe sequences and that of the target nucleic acid. Some previous studies have demonstrated that the inconsistencies between tested sequences and primers or probes might affect the amplification efficiency or the sensitivity of detection [11, 21]; however, the exact number and positions of mismatches leading to detection failure has not been determined [21]. The likelihood of a detection failure is highest if the mismatch is at the center of the probe or if a total of four mismatches are present in the primer or probe [11]. Thus, when considering the design of an ideal primer or probe, it may be beneficial to optimize the primer and probe sequences according to those of the major endemic strain populations, which was the approach taken in this study. The selected primer and probe sequences showed complete identity with 85.7% of the sequences from the published strains; only 11.1% of the sequences possessed one mismatch in the primers. Of all the published RABV-TWFB N gene sequences [4, 18], only the KP860178 sequence had a mismatch at the center of the probe, which may or may not have affected the nucleic acid detection of this strain using our platform.

According to phylogenetic analysis, RABV-TWFB may have been present in Taiwan for many decades [4]; however, no human cases were ever reported. Nevertheless, it is necessary to develop sensitive diagnostic techniques based on the detection of conserved nucleic acid sequences of locally endemic viruses as a public health precaution, in case a human case should be reported. Early diagnosis from peripheral tissues will alleviate the

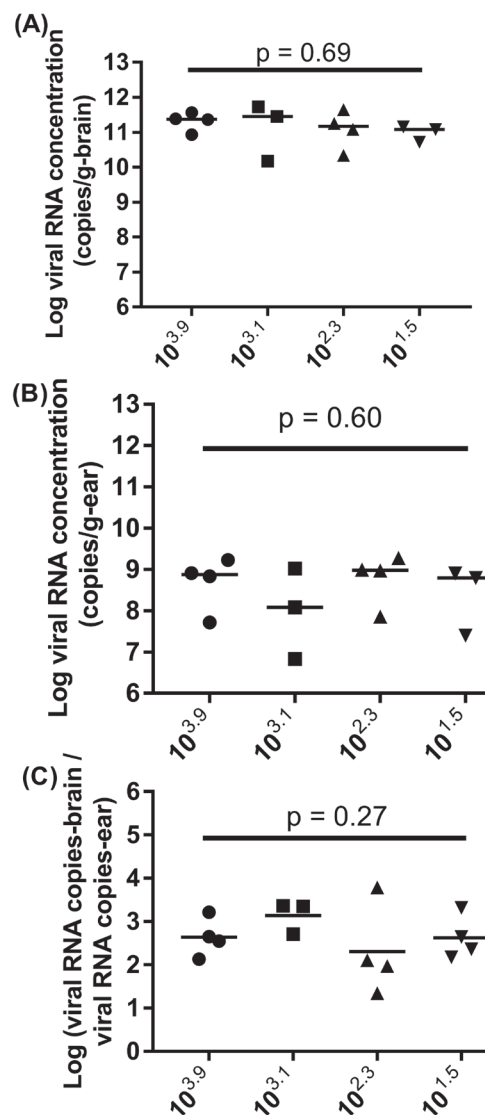


Fig. 4. Quantification and comparison of viral RNA concentrations extracted from brain and ear specimens from ferret badgers. Viral RNA concentrations derived from brain (A) and ear (B) specimens of ferret-badgers and the ratio of viral RNA concentration in brain/ear samples (C) were compared according to the amount of virus used to inoculate the ferret badgers ($10^{3.9}$, $10^{3.1}$, $10^{2.3}$ and $10^{1.5}$ MICLD₅₀ of RABV-TWFB). The X-axis represents the groups receiving a different virus load. The line in each group is the median (A) and mean (B) value of the RNA copy-number concentration, or median ratio (C). The solid circle, square, triangle, and reverse triangle icons are the values from each animal in each group. The statistical analysis revealed no significant differences in either median RNA concentrations derived from brain specimens or mean RNA concentrations derived from ear specimens. In addition, no significant differences were observed in the ratios of viral RNA concentration from brain/ear samples for groups of animals that received different virus loads of $10^{1.5}$ – $10^{3.9}$ MICLD₅₀.

concern of accidental exposure of medical personnel, and may also be used as a screening test prior to organ transplantation.

The present study revealed significant RNA disparities between the LOD of our technique and viral loads from the ear specimens, which clearly displayed satisfactory sensitivity for rabies diagnosis. This method may replace other post-mortem diagnostic techniques for Taiwan ferret badger rabies after further reliable and extensive evaluations on field samples are completed. The use of ear tissues associated with nucleic acid-based diagnostic techniques would greatly simplify procedures and avoid the need of highly specialized facilities for rabies diagnosis. We hope that this study will stimulate innovative thinking for rabies diagnosis based on ear sampling and nucleic-acid detection as an alternative to the post-mortem examination currently used for rabies diagnosis.

ACKNOWLEDGMENTS. This study was financially supported by the Bureau of Animal and Plant Health Inspection and Quarantine, Council of Agriculture, Executive Yuan, Taiwan (R.O.C.) (grant nos. MOST 103-3114-Y-518-001, MOST 104-3114-Y518-002, and 1052101011001-101005B2). The authors would like to thank Dr. Jyh-Mirn Lai from National Chia yi University and Dr. Ya-Jane Lee from National Taiwan University for their guidance on the statistical analysis.

REFERENCES

1. Animal Health Research Institute 2013. AHRI The full genome sequences of rabies virus from Formosan ferret badger in Taiwan. <http://www.nvri.gov.tw/module/NewsContent/400/392.aspx?nid=%2b7kpxBWw0%3d&type=z04176wykT8%3d> [accessed on August 30, 2016].
2. Black, E. M., Lowings, J. P., Smith, J., Heaton, P. R. and McElhinney, L. M. 2002. A rapid RT-PCR method to differentiate six established genotypes of rabies and rabies-related viruses using TaqMan technology. *J. Virol. Methods* **105**: 25–35. [Medline] [CrossRef]
3. Bureau of Animal and Plant Health Inspection and Quarantine 2016. BAPHIQ Results of Rabies epidemics surveillance. <http://www.baphiq.gov.tw/view.php?catid=10980> [accessed on March 31, 2018].
4. Chiou, H. Y., Hsieh, C. H., Jeng, C. R., Chan, F. T., Wang, H. Y. and Pang, V. F. 2014. Molecular characterization of cryptically circulating rabies virus from ferret badgers, Taiwan. *Emerg. Infect. Dis.* **20**: 790–798. [Medline] [CrossRef]
5. Cliquet, F., Aubert, M. and Sagné, L. 1998. Development of a fluorescent antibody virus neutralisation test (FAVN test) for the quantitation of rabies-neutralising antibody. *J. Immunol. Methods* **212**: 79–87. [Medline] [CrossRef]
6. Cliquet, F., Picard-Meyer, E. and Robardet, E. 2014. Rabies in Europe: what are the risks? *Expert Rev. Anti Infect. Ther.* **12**: 905–908. [Medline] [CrossRef]
7. Crepin, P., Audry, L., Rotivel, Y., Gacoin, A., Caroff, C. and Bourhy, H. 1998. Intravitam diagnosis of human rabies by PCR using saliva and cerebrospinal fluid. *J. Clin. Microbiol.* **36**: 1117–1121. [Medline]
8. Dacheux, L., Reynes, J. M., Buchy, P., Sivuth, O., Diop, B. M., Rousset, D., Rathat, C., Jolly, N., Dufourcq, J. B., Nareth, C., Diop, S., Iehlé, C., Rajerison, R., Sadorge, C. and Bourhy, H. 2008. A reliable diagnosis of human rabies based on analysis of skin biopsy specimens. *Clin. Infect. Dis.* **47**: 1410–1417. [Medline] [CrossRef]
9. Dyer, J. L., Yager, P., Orciari, N., Greenberg, L., Wallace, R., Hanlon, C. A. and Blanton, J. D. 2014. Rabies surveillance in the United States during 2013. *J. Am. Vet. Med. Assoc.* **245**: 1111–1123. [Medline] [CrossRef]
10. Fooks, A. R., Johnson, N., Freuling, C. M., Wakeley, P. R., Banyard, A. C., McElhinney, L. M., Marston, D. A., Dastjerdi, A., Wright, E., Weiss, R. A. and Müller, T. 2009. Emerging technologies for the detection of rabies virus: challenges and hopes in the 21st century. *PLoS Negl. Trop. Dis.* **3**: e530. [Medline] [CrossRef]
11. Hughes, G. J., Smith, J. S., Hanlon, C. A. and Rupprecht, C. E. 2004. Evaluation of a TaqMan PCR assay to detect rabies virus RNA: influence of sequence variation and application to quantification of viral loads. *J. Clin. Microbiol.* **42**: 299–306. [Medline] [CrossRef]
12. Koprowski, H. 1996. The mouse inoculation test. pp. 80–86. *In: Laboratory Techniques in Rabies*, 4th ed. (Meslin, F. X., Kaplan, M. M. and Koprowski, H. eds.), World Health Organization, Geneva.
13. Macedo, C. I., Carnieli, P. Jr., Brandão, P. E., Travassos da Rosa, E. S., Oliveira, R. N., Castilho, J. G., Medeiros, R., Machado, R. R., Oliveira, R. C., Carrieri, M. L. and Kotait, I. 2006. Diagnosis of human rabies cases by polymerase chain reaction of neck-skin samples. *Braz. J. Infect. Dis.* **10**: 341–345. [Medline] [CrossRef]
14. Mani, R. S. and Madhusudana, S. N. 2013. Laboratory diagnosis of human rabies: recent advances. *Sci. World J.* **2013**: 569712. [Medline] [CrossRef]
15. Panning, M., Baumgarte, S., Pfeifferle, S., Maier, T., Martens, A. and Drosten, C. 2010. Comparative analysis of rabies virus reverse transcription-PCR and virus isolation using samples from a patient infected with rabies virus. *J. Clin. Microbiol.* **48**: 2960–2962. [Medline] [CrossRef]
16. Picard-Meyer, E., Bruyère, V., Barrat, J., Tissot, E., Barrat, M. J. and Cliquet, F. 2004. Development of a hemi-nested RT-PCR method for the specific determination of European Bat Lyssavirus 1. Comparison with other rabies diagnostic methods. *Vaccine* **22**: 1921–1929. [Medline] [CrossRef]
17. Smith, J., McElhinney, L., Parsons, G., Brink, N., Doherty, T., Agranoff, D., Miranda, M. E. and Fooks, A. R. 2003. Case report: rapid ante-mortem diagnosis of a human case of rabies imported into the U.K. from the Philippines. *J. Med. Virol.* **69**: 150–155. [Medline] [CrossRef]
18. Tsai, K. J., Hsu, W. C., Chuang, W. C., Chang, J. C., Tu, Y. C., Tsai, H. J., Liu, H. F., Wang, F. I. and Lee, S. H. 2016. Emergence of a sylvatic enzootic formosan ferret badger-associated rabies in Taiwan and the geographical separation of two phylogenetic groups of rabies viruses. *Vet. Microbiol.* **182**: 28–34. [Medline] [CrossRef]
19. Wacharapluesadee, S. and Hemachudha, T. 2002. Urine samples for rabies RNA detection in the diagnosis of rabies in humans. *Clin. Infect. Dis.* **34**: 874–875. [Medline] [CrossRef]
20. Wacharapluesadee, S. and Hemachudha, T. 2010. Ante- and post-mortem diagnosis of rabies using nucleic acid-amplification tests. *Expert Rev. Mol. Diagn.* **10**: 207–218. [Medline] [CrossRef]
21. Wacharapluesadee, S., Sutipanya, J., Damrongwatanapokin, S., Phummesin, P., Chamnanpood, P., Leowijuk, C. and Hemachudha, T. 2008. Development of a TaqMan real-time RT-PCR assay for the detection of rabies virus. *J. Virol. Methods* **151**: 317–320. [Medline] [CrossRef]
22. Webster, W. A. and Casey, G. A. 1996. Virus isolation in neuroblastoma cell culture. pp. 96–103. *In: Laboratory Techniques in Rabies*, 4th ed. (Meslin, F. X., Kaplan, M. M. and Koprowski, H. eds.), World Health Organization, Geneva.
23. World Health Organization 2013. WHO Rabies; Chinese Taipei. Weekly Disease Information. http://www.who.int/wahis_2/public/wahid.php/Reviewreport/Review?page_refer=MapFullEventReport&reportid=13775 [accessed on July 7, 2014].
24. World Organization for Animal Health 2013. OIE Manual of Diagnostic Tests and Vaccines for Terrestrial Animals. http://www.oie.int/fileadmin/Home/eng/Health_standards/tahm/2.01.17_RABIES.pdf [accessed on January 3, 2017].
25. Zieger, U. 2015. Diagnosis of Rabies via RT-PCR on Skin Samples of Wild and Domestic Animals. *Open J. Vet. Med.* **5**: 191–196. [CrossRef]